Electropolymerized Films of Macromeric Assemblies

Toru Kajita,† Robert M. Leasure, Martin Devenney, Duane Friesen, and Thomas J. Meyer*

Kenan Laboratories of Chemistry, The University of North Carolina at Chapel Hill, Venable Hall, CB# 3290, Chapel Hill, North Carolina 27599-3290

Received October 10, 1997

The polymer poly[4-(2-aminoethyl)styrene], prepared by living anionic polymerization, has been derivatized by amide coupling to $[Ru^{II}(vbpy)_2(4\text{-}CO_2H\text{-}4'\text{-}CH_3bpy)]^{2+}$ (vbpy is 4-vinyl-4′-methyl-2,2′-bipyridine; $4\text{-}CO_2H\text{-}4'\text{-}CH_3bpy$ is 4-methyl-2,2′-bipyridine-4′-carboxylic acid). The resulting "macromer" can be electropolymerized on a variety of electrode materials by reductive electropolymerization. Compared to similar films of poly$[Ru^{II}(vbpy)_3](PF_6)_2$: (1) the macromeric films are considerably rougher, apparently having open, local microporous structures; (2) they undergo comparable rates of intrafilm charge transfer; and (3) they have shortened metal-to-ligand charge transfer (MLCT) excited state lifetimes, apparently due to quenching by film-based trap sites. Stable films of a mixed polymer have also been prepared by sequential addition of $[Ru^{II}(bpy)_2(4\text{-}CO_2H\text{-}4'\text{-}CH_3bpy)]^{2+}$ and then the vbpy derivative.

Introduction

There are well-established procedures for preparing redox-active, metallopolymeric films at electrode surfaces.[1] One involves electropolymerization of transition metal complexes containing polymerizable ligand substituents, such as vinyl[2,3] or pyrrole.[4−6] For example, electrochemical reduction of $[Ru^{II}(vbpy)_3]^{2+}$ (vbpy is 4-vinyl-4′-methyl-2,2′-bipyridine) leads to the formation of cross-linked, electroactive, network polymers which are quite stable.[2,7]

One of our current research interests is extending the underlying interfacial synthetic chemistry to more complex molecules and to molecular assemblies. In this study we describe the electropolymerization of a macromolecular monomer or "macromer",[8,9] which contains polypyridyl Ru^{II} complexes. The parent polymer, poly[4-(2-aminoethyl)styrene], was prepared by using living anionic polymerization techniques to give controlled molecular weights and narrow polydispersities. The polymer was derivatized by amide coupling with $[Ru^{II}(vbpy)2(4\text{-}CO_2\text{-}4'\text{-}CH_3bpy)]^{2+}$ ($4\text{-}CO_2\text{-}4'\text{-}CH_3bpy$ is 4-methyl-2,2′-bipyridine-4′-carboxylic acid) based on well-established amino acid coupling chemistry.[10−12] A repeat unit of the derivatized polymer and the formula used to abbreviate it are shown (**1**).

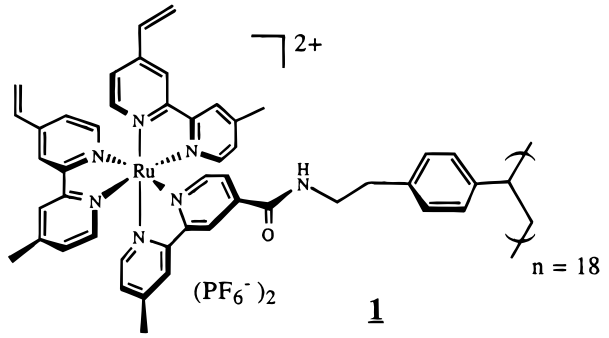

1

$\{p\text{-}PS\text{-}CH_2CH_2NHCO\text{-}[bRu^{II}(vbpy)_2]_{18}\}(PF_6)_{36}$

Experimental Section

Materials. 4-(Chloromethyl)styrene (Eastman Chemical) was purified on a basic alumina column by eluting with freshly distilled diethyl ether to remove the commercially added radical inhibitor (4-*tert*-butylcatechol, 500, μg/g). Lithium bis(trimethylsilyl)amide (1.0 M in hexane), chloromethyl methyl ether, *sec*-butyllithium (1.3 M in cyclohexane), 4-methylmorpholine (NMM), 4-(dimethylamino)pyridine (DMAP), 2-phenethylamine, ammonium hexafluorophosphate, and methyltrimethoxysilane (MTMS) were reagent grade (Aldrich) and used as received. The concentration of the *sec*-butyllithium solution was determined by using the Gilman double-titration method.[13] (Benzo-

* To whom correspondence should be addressed.
† Current address: Japan Synthetic Rubber Co., Ltd., 100 Kawajiri-cho, Yokkaichi, Mie 510 Japan.

(1) Molecular Design of Electrode Surfaces; Murray, R. W., Ed.; John Wiley & Sons, Inc.: New York, 1992; Vol. XXII.
(2) Denisevich, P.; Abruña, H. D.; Leidner, C. R.; Meyer, T. J.; Murray, R. W. *Inorg. Chem.* **1982**, *21*, 2153−2161.
(3) Calvert, J. M.; Schmehl, R. H.; Sullivan, B. P.; Facci, J. S.; Meyer, T. J.; Murray, R. W. *Inorg. Chem.* **1983**, *22*, 2151−2162.
(4) Cosnier, S.; Deronzier, A.; Moutet, J.-C. *J. Phys. Chem.* **1985**, *89*, 4895−4897.
(5) Downard, A. J.; Surridge, N. A.; Meyer, T. J. *J. Electroanal. Chem.* **1988**, *246*, 321−335.
(6) Deronzier, A.; Moutet, J.-C. *Acc. Chem. Res.* **1989**, *22*, 249−255; *Coord. Chem. Rev.* **1996**, *147*, 335−376.
(7) Ikeda, T.; Schmehl, R.; Denisevich, P.; Willman, K.; Murray, R. W. *J. Am. Chem. Soc.* **1982**, *104*, 2683−2691.
(8) The term macromer was originally a registered trademark of CPC International but is now commonly applied to organic polymers containing end-chain functional groups that can undergo further polymerization.
(9) Encyclopedia of Polymer Science and Engineering; Kroschwitz, J. I., Ed.; John Wiley & Sons: New York, 1987; Vol. 9.
(10) Peek, B. M.; Ross, G. T.; Edwards, S. W.; Meyer, G. J.; Meyer, T. J.; Erickson, B. W. *Int. J. Pept. Protein Res.* **1991**, *38*, 194.
(11) Mecklenburg, S. L.; Peek, B. M.; Schoonover, J. R.; McCafferty, D. G.; Wall, C. G.; Erickson, B. W.; Meyer, T. J. *J. Am. Chem. Soc.* **1993**, *115*, 5479−5495.
(12) McCafferty, D. G.; Bishop, B. M.; Wall, C. G.; Hughes, S. G.; Mecklenberg, S. L.; Meyer, T. J.; Erickson, B. W. *Tetrahedron* **1995**, *51*, 1093−1106.
(13) Gilman, H.; Cartledge, F. K. *J. Organomet. Chem.* **1964**, *2*, 447−454.

S0020-1669(97)01279-2 CCC: $15.00
Published on Web 09/01/1998

triazol-1-yloxy)tris(dimethylamino)phosphonium hexafluorophosphate (BOP) and 1-hydroxybenzotriazole hydrate (HOBT) were used as received (Nova Biochem). Tetrahydrofuran (THF) and diethyl ether (Et_2O) were distilled under argon from sodium/benzophenone. Dimethylformamide (DMF, Fisher Certified Grade) was dried over 4 Å molecular seives. Methanol (MeOH, Mallinckrodt) and acetonitrile (Burdick and Jackson, UV spectra grade) were used as received. $[Ru^{II}(bpy)_3](PF_6)_2$,[14] $[Os^{II}(dmb)_3](PF_6)_2$ (dmb is 4,4′-dimethyl-2,2′-bipyridine),[15] $Ru^{II}(vbpy)_3](PF_6)_2$,[2] $Ru^{II}(vbpy)_2Cl_2 \cdot 2H_2O$,[16] 4-methyl-2,2′-bipyridine-4′-carboxylic acid (4-CO_2H-4′-CH_3bpy),[10,12] and $[Ru^{II}(bpy)_2$(4-CO_2H-4′-CH_3bpy)$](PF_6)_2$[10,12] were prepared according to literature procedures. In the peptide coupling reactions, dry DMF solutions of BOP (4.6 wt %), HOBT (3.2 wt %), NMM (5.1 wt %), and DMAP (3.3 wt %) were freshly prepared just prior to use.

Electrochemical measurements were performed in acetonitrile (Burdick and Jackson, UV spectra grade) which was bubble degassed and stored under nitrogen. The supporting electrolyte was tetra-*n*-butylammonium hexafluorophosphate (TBAH) or lithium perchlorate (GFS Chemicals) which had been purified by recrystallization as described elsewhere.[17,18]

Equipment and Instrumentation. ^1H and ^{13}C NMR spectra were acquired with a 200 MHz Brücker AC200 spectrometer in $CDC1_3$, CD_3OD, or CD_3CN (Cambridge Isotopes).

Gel permeation chromatography (GPC) was performed on a Waters 150-CV GPC with Ultrastyragel (cross-linked polystyrene) columns of 100, 500, 103, 104, and 105 A porosities, tetrahydrofuran as the eluent, and polystyrene standards (Showa Denko).

Infrared spectra were collected with a Mattson Instruments Inc. Galaxy Series 5000 FTIR spectrometer. Transmission infrared spectra were collected from KBr pellets with a triglycine sulfate pyroelectric (TGS) detector. Specular reflectance infrared spectra were acquired by using a liquid nitrogen cooled mercury cadmium telluride (MCT) detector and a grazing angle attachment (Herrick Scientific Corp.) with an angle of incidence fixed at 75°.

Voltammetric and chronoamperometric experiments were carried out by using a Princeton Applied Research model 273 potentiostat/galvanostat interfaced to an IBM compatible PC. Rotating disk voltammetry was performed by using a Pine Instruments Co. model ASR rotator and ASRP speed controller. Electrochemical experiments were carried out in acetonitrile solutions containing 0.1 M TBAH or 1.0 M $LiClO_4$ as the supporting electrolyte with a nonaqueous Ag/$AgNO_3$ reference electrode (0.31 ± 0.03 V vs SSCE).[18] Electropolymerizations were carried out in a Vacuum Atmospheres glovebox modified to operate under a constant N_2 purge. Two-compartment electrochemical cells were designed such that a platinum mesh counter electrode was reproducibly positioned parallel to and opposite the working electrode. This arrangement provided a uniform current density over the entire surface of the working electrode, allowing for more homogeneous film growth.

Rotated disk and cyclic voltammetry measurements were conducted on Teflon-shrouded platinum disk electrodes (~0.12 cm^2) which had been polished prior to use with 1 μm diamond paste (Buehler). For SEM and FTIR studies, electrodes of Au/Cr/SiO_2 were prepared by vapor deposition of a gold layer (~2000 Å) over an adhesive layer of chromium (~200 Å) on glass with locally built equipment which applied resistive electrical heating at reduced pressure (2×10^{-5} Torr). For AFM measurements, electrodes were fashioned from pieces of freshly cleaved, highly oriented pyrolytic graphite (HOPG, Union Carbide pyrolytic graphite monochromator ZYA).[18] For photophysical measurements, films were grown on optically transparent electrodes of tin-doped indium oxide (ITO) coated on glass (Delta Technologies, Ltd.), as described elsewhere.[18]

Scanning electron microscopy (SEM) was performed by using an Etec Autoscan SEM operating at an accelerating voltage of 20 kV. Prior to analysis, samples were coated with 200−300 Å of a gold/palladium alloy in a Polaron 5100 plasma sputter coater. Atomic force microscopy images were aquired with a Nanoscope III (Digital Instruments, Inc.) equipped with a silicon tip and operating in the "tapping mode" at a resonant frequency of ~360 kHz. Root-mean-square (rms) roughness values were determined by using Nanoscope III software. X-ray photoelectron spectroscopy (XPS) was performed by using a Perkin-Elmer Electronics model 5400 XPS instrument. The operating conditions were as follows: Mg Kα anode (15 kV, 400 W); hemispherical analyzer (pass energy 35 eV); angle of collection 45°; analysis area 0.031 mm^2; base pressure 1×10^{-8} Torr. Binding energies were charge referenced to the C 1 s photoelectron peak at 285.0 eV. Photoelectron spectra were analyzed by using a standard curve-fit routine (80% Gaussian and 20% Lorentzian) with a Shirley background subtraction.[19] UV−vis spectra were aquired by using a Hewlett-Packard 8452A photodiode-array spectrometer for polymeric films; light scattering effects were minimized by including a clean ITO electrode in the reference scan. Steady state emission measurements were made on a SPEX Fluorolog 212A spectrofluorimeter interfaced to a Z-80 based DM1B computer running the CP/M operating system.[18]

Time-resolved emission measurements were made by using a PRA LN1000/LN102 nitrogen laser/dye laser combination for excitation (λ = 457 nm, Coumarin 460) operating at 90 $\mu J/cm^2$ per pulse for solution samples and 5−25 $\mu J/mm^2$ per pulse for film samples. Emission was monitored at right angles by using a Macpherson 272 monochromator and a Hamamatsu R3896 photomultiplier tube. As with steady state emission measurements, film samples on ITO electrodes were positioned at an angle of ~60° relative to the normal of the excitation source in order to maximize the collected emission signal.

Syntheses. [*N*,*N*-Bis(trimethylsilyl)amino]methyl Methyl Ether (2). To a 500 mL round bottom flask containing chloromethyl methyl ether (20 mL, 0.263 mol) at 0 °C under an argon atmosphere was added 250 mL of a 1.0 M THF solution of lithium bis(trimethylsilyl)amide (0.25 mol) over a period of 10 min. Precipitation of lithium chloride was observed during the addition. The reaction mixture was stirred for an additional 14 h at room temperature. The LiCl was removed by filtration. The filtrate was distilled under argon at ambient pressure to remove the THF, and then at reduced pressure to obtain [*N*,*N*-bis(trimethylsilyl)amino]methyl methyl ether as a colorless liquid (bp 74 °C at 24 mmHg). Yield: 86%. The product was stored under argon, and freshly distilled prior to use. ^1H NMR (δ (ppm), $CDCl_3$): 4.26 (s, 2H, $-CH_2-$), 3.15 (s, 3H, CH_3), 0.11 (s, 18H, $SiMe_3$).

4-{2-[*N*,*N*-bis(trimethylsilyl)amino]ethyl}styrene (3). Into a dry Et_2O suspension of magnesium powder (5.0 g, 0.206 mol) at 0 °C under an argon atmosphere in a 250 mL, three-necked round bottom flask equipped with rubber septa and a condenser was added 50 mL of a dry Et_2O solution of 4-(chloromethyl)styrene (20 g, 0.131 mol) via a syringe. The reaction mixture immediately turned dark green due to the exothermic formation of the Grignard reagent, (4-vinylbenzyl)-magnesium chloride. It was stirred for 30 min while cooling in an ice bath, and then for an additional 1 h while heating at reflux. After cooling of the reaction mixture in an ice bath, freshly distilled [*N*,*N*-bis(trimethylsilyl)amino]methyl methyl ether (**2**) (28 g, 0.136 mol) was added over a period of 5 min, resulting in the gradual disappearance of the green color and the formation of a colorless precipitate. The mixture was stirred for 14 h at room temperature. The precipitate and unreacted magnesium were removed by filtration, and the filtrate was washed with three aliquots of distilled water. The nonaqueous layer was evaporated by using a rotary evaporator to yield a viscous yellow oil. Distillation at reduced pressure yielded 4-{2-[*N*,*N*-bis(trimethylsilyl)-amino]ethyl}styrene (**3**) as a colorless liquid, bp 142−144 °C at 4.0 mmHg (lit. bp 105−110 °C at 0.98 mmHg).[20] Yield: 42%, 16.0 g. ^1H NMR (δ (ppm), $CDC1_3$): 6.81−7.25 (m, 4H, aromatic), 6.57 (dd, J_{AX}

(14) Caspar, J. V.; Meyer, T. J. *J. Am. Chem. Soc.* **1983**, *105*, 5583−5590.
(15) Terrill, R. H.; Sheehan, P. E.; Long, V. C.; Washburn, S.; Murray, R. W. *J. Phys. Chem.* **1994**, *98*, 5127−5134.
(16) Leasure, R. M.; Ou, W.; Moss, J. A.; Linton, R. W.; Meyer, T. J. *Chem. Mater.* **1996**, *8*, 264−273.
(17) Perin, D. D.; Armarego, W. L. F. *Purification of Laboratory Chemicals*, 3rd ed.; Pergamon Press: Oxford, 1992.
(18) Leasure, R. M. Ph.D. Dissertation, University of North Carolina, 1995.
(19) Shirley, D. A. *Phys. Rev. B* **1972**, *5*, 4709−4714.
(20) Suzuki, K.; Hirao, A.; Nakahama, S. *Makromol. Chem.* **1989**, *190*, 2893−2901.

= 17.2 Hz and J_{BX} = 11.3 Hz, 1H, H_X), 5.53 (d, J_{XA} = 17.8 Hz, 1H, H_A), 5.05 (d, J_{XB} = 10.8 Hz, 1H, H_B), 2.60−3.02 (m, 4H, $-CH_2CH_2-$), 0.01 (s, 18H, $SiMe_3$)

Poly(4-{2-[*N*,*N*-bis(trimethylsilyl)amino]ethyl}styrene) (4). Reaction glassware was washed with a 1:1 mixture of nitric acid and concentrated sulfuric acid, thoroughly rinsed with distilled water, and dried overnight in an electric oven. Before addition of the reactants, a 100 mL one-necked round bottom flask was sealed with a rubber septum and heated with a heat gun while the flask was being purged with a stream of argon through two needles inserted into the septum. All subsequent operations were conducted under an argon atmosphere. The styrene monomer (**3**) (4.64 g, 15.9 mmol) and 40 mL of THF were added to the reaction flask via syringe. The solution was cooled to −78 °C in a dry ice/acetone bath while being stirred. Polymerization was initiated by the addition of *sec*-butyllithium (0.60 mL of a 1.31 M solution in cyclohexane, 0.762 mmol) via a microsyringe and was accompanied by a characteristic color change from colorless to green, typical of living anionic polymerizations. The solution was stirred for 30 min at −78 °C. The polymerization was terminated by the addition of deoxygenated methanol. The polymer was obtained as a colorless precipitate by addition of excess methanol and purified by recrystallizing three times from THF/MeOH. Yield: ca. 100%. The product was stored in vacuo. ^{1}H NMR (δ (ppm), $CDCl_3$): 6.2−7.0 (m, 4H, aromatic), 3.95 (m br, 2H, $-NCH_2-$), 2.55 (m br, 2H, $-PhCH_2-$), 1.0−1.8 (m br, 3H, $-CH_2CHR-$), 0.7 (s, 18H, $SiMe_3$). ^{13}C NMR (δ (ppm), $CDCl_3$): 143.2 (m, aromatic C-4), 137.2 (m, aromatic C-1), 127.6 (m, aromatic C-2, C-3, C-6), 48.1 (s, $-N-CH_2-$ side chain), 42 (s, $-PhCH_2-$ side chain), 40.5 (m, $-CHRCH_2-$ main chain). GPC ($\bar{M}_n$ (calcd) = 5950): $\bar{M}_w$ = 5940, $\bar{M}_n$ = 5350, $\bar{M}_w/\bar{M}_n$ = 1.10.

Poly[4-(2-aminoethyl)styrene] (5). To a stirred solution of the trimethylsilyl-capped polymer (**4**) (1.0 g) in 25 mL of THF at room temperature was added 1 mL of concentrated HCl over a period of 5 min. The solution was stirred for an additional 1 h and then evaporated to obtain the colorless solid, poly[4-(2-aminoethyl)styrene hydrochloride]. The hydrochloride polymer was dissolved in 25 mL of methanol and precipitated as poly[4-(2-aminoethyl)styrene] by dropwise addition to 100 mL of a stirred dioxane solution of KOH (10 wt %). The precipitate was filtered and washed with copious volumes of distilled water and diethyl ether to remove residual bis(trimethylsilyl) ether and dry the polymer. The product was stored in a vacuum desiccator in the presence of NaOH to scavenge CO_2. Reaction of the amine groups with CO_2 leads to the carbonamide-modified polymer. The polymer can be recovered in the amine form by treatment with HCl and KOH as described above. Yield: ca. 100%. ^{1}H NMR (δ (ppm), CD_3OD): 6.27−7.08 (m br, 4H, aromatic), 2.52−2.97 (m br, 4H, $-CH_2CH_2-$), 0.8−2.0 (m br, $-CH_2CHR-$main chain). The resonance for the amine protons was not observed due to H−D exchange. ^{13}C NMR (δ (ppm), CD_3OD): 142−145 (m, aromatic, C-4), 137.3 (m, aromatic C-1), 128.1 (m, aromatic C-2, C-3, C-5, C-6), 47.7 (s, $-NCH_2-$ side chain), 42.0 (s, $-PhCH_2-$ side chain), 40.3 (m, $-CHRCH_2-$ main chain). FTIR (KBr): 1902, 1641 (br), 1596 (br), 1510, 1441, 1419, 1381, 1353, 1317, 1184, 1113, 1070, 1019, 815 (br), 567 (br).

$[Ru^{II}(vbpy)_2(4\text{-}CO_2H\text{-}4'CH_3bpy)](PF_6)_2$ (6). In a 250 mL round bottom flask equipped with a condenser was heated a stirred suspension of $Ru^{II}(vbpy)_2Cl_2\cdot 2H_2O$ (270 mg, 0.45 mmol) and 4-methyl-2,2′-bipyridine-4′-carboxylic acid (4-CO_2H-4′-CH_3bpy/107 mg, 0.50 mmol) in 100 mL of 70% EtOH/H_2O at reflux under an argon atmosphere for 6 h. Over the course of the reaction, the purple reaction mixture turned into a red, homogeneous solution. The solution was cooled to room temperature and the ethanol removed by rotary evaporation. The complex was precipitated from the remaining aqueous solution by acidification with 3 mL of concentrated HCl and addition of 5 mL of a concentrated aqueous NH_4PF_6 solution. The precipitate was collected on a fine glass frit and washed with distilled water (2 × 15 mL) and diethyl ether (3 × 30 mL). It was purified on an ion-exchange resin column of Sephadex-CM C-25 by eluting with an aqueous solution of 0.1 M NH_4Cl and phosphate buffer, pH 7.0. The complex was again precipitated as the PF_6^- salt by acidification with 3 mL of concentrated HCl and addition of 5 mL of concentrated aqueous NH_4PF_6. The product was collected as an orange/red amorphous powder by filtration on a fine glass frit and washed with cold distilled water and diethyl ether. Yield: 110 mg, 24%. ^{1}H NMR (δ (ppm), CD_3CN): 8.89 (s, 1 H. aromatic), 8.32−8.51 (m, 5 H, aromatic), 7.10−7.89 (m, 12 H, aromatic), 6.70−6.95 (m, 2 H, H_X), 6.32−6.57 (m, 2 H, H_A), 5.6−5.77 (m, 2 H, H_B), 2.2−2.8 (m, 9 H, CH_3). FTIR (KBr): 3427 (br), 3118, 3085, 2926, 2854, 1718, 1618, 1540, 1480, 1426, 1301, 1237, 840, 557 cm^{-1}. UV−vis (CH_3CN): λ_{max} (ϵ_{rel}) = 248 (0.762), 296 (1.00), 466 (0.295) nm. ϵ_{rel} values are the calculated extinction coefficients relative to 296 nm. Anal. Calcd for $C_{38}H_{34}F_{12}N_6O_2P_2Ru$: C, 45.74; H, 3.43; N, 8.42. Found: C, 45.6; H, 3.6; N, 8.3.

Macromer. {p-PS-$CH_2CH_2NHCO[-bRu^{II}(vbpy)_2]_{18}$}$(pF_6)_{36}$ (1). Into a 50 mL round bottom flask were added dry DMF (5.7 g), poly-[4-(2-aminoethyl)styrene] (**5**) (21.0 mg, 0.143 mmol $-NH_2$), $[Ru^{II}(vbpy)_2(bpy\text{-}COOH)](PF_6)_2$ (**6**) (200 mg, 0.218 mmol), BOP solution (2.06 g, 0.215 mmol), HOBT solution (1.03 g, 0.215 mmol), NMM solution (0.45 g, 0.217 mmol), and DMAP solution (0.80 g, 0.215 mmol). The reaction mixture was stirred at room temperature for 12 h and then added dropwise into 200 mL of dry Et_2O to form an orange precipitate. The precipitate was collected on a fine glass frit by filtration, dissolved in 10 mL of acetonitrile, and added dropwise to 100 mL of an aqueous sodium bicarbonate solution (10 wt %) to again form an orange precipitate. The precipitate was collected on a fine glass frit and washed with copious volumes of distilled water. Initially, an orange filtrate was observed due to unbound metal complex **6**. Precipitations from acetonitrile solutions into Et_2O and aqueous $NaHCO_3$ were continued until no absorption band could be detected in the UV−vis absorption spectrum of the aqueous filtrates. Unreacted amino groups were capped with acetylamide groups by stirring the precipitate in 30 mL of a 1:1 acetic anhydride/acetonitrile solution at 50 °C for 2 h. The product was precipitated by dropwise addition into excess Et_2O, filtered, washed with several aliquots of Et_2O, and dried in vacuo. The ruthenium-loaded polymer salt 1 was obtained as an amorphous, orange solid; yield ∼60%. The reaction proceeded essentially to completion. The low percent yield is a consequence of the numerous reprecipitations and filtrations necessary to purify the macromer. ^{1}H NMR (δ (ppm), CD_3CN): 6.2−8.9 (m br, 24 H, aromatic and H_X),5.15 (m, H_A, 2H), 6.05 (m, H_B, 2H), 2.7−3.5 (m, br, $-CH_2CH_2-$ side chain, 2H), 0.4−2.7 (m, $-CONHCH_2CH_2-$, methyl, *sec*-Bu, $-(CH_2CHR)-$ main chain). FTIR (KBr): 3081, 3031, 2958, 2925, 2875, 2852, 1652, 1618, 1539, 1478, 1428, 1237, 843, 557 cm^{-1}. UV−vis (CH_3CN): λ_{max} (ϵ_{rel}) = 248 (0.787), 296 (1.00), 468 (0.387) nm. Anal. Calcd for $C_{48}H_{45}F_{12}N_7OP_2Ru$ for the repeating unit: C, 51.2; H, 4.0; N, 8.7. Found: C, 52.3; H, 4.6; N, 7.8.

Mixed-Complex Macromer {p-PS-$CH_2CH_2NHCO[-bRu^{II}(vbpy)_2]_{2.7}[-bRu^{II}(bpy)_2]_{15.3}$}$(PF_6)_{36}$ (7). The partially loaded macromolecule {p-PS-$CH_2CH_2NHCO[-bRu^{II}(bpy)_2]_{14.5}$}$(PF_6)_{14.5}$ was prepared by coupling poly-[4-(2-aminoethyl)styrene] (14 mg, 0.095 mmol, 1 equiv) and $[Ru^{II}(bpy)_2(4\text{-}CO_2H\text{-}4'\text{-}CH_3bpy)](PF_6)_2$ (80 mg, 0.080 mmol, 0.85 equiv) with ca. 1.4 equiv of each peptide coupling reagent and the reaction conditions described for the preparation of **1**. A small portion of the partially loaded macromolecule was capped as the acetylamide, as described above, in order to determine the extent of loading of the first complex by ^{1}H NMR analysis.[21,22] The remainder (40 mg, ca. 9.2 μmol) was allowed to react with excess **6** (50 mg, 0.05 mmol) to couple with the free amine sites. The polymer was purified as before by successive reprecipitations from CH_3CN into Et_2O and aqueous $NaHCO_3$.

$[Ru^{II}(vbpy)_2(4\text{-}CH_3\text{-}4'\text{-}(CONHCH_2CH_2Ph)bpy)](PF_6)_2$ (8). Into a 50 mL round bottom flask were added dry DMF (5.7 g), 2-phenethylamine (17.3 mg, 0.143 mmol), **6** (200 mg, 0.218 mmol), BOP solution (2.06 g, 0.215 mmol), HOBT solution (1.03 g, 0.215 mmol), NMM solution (0.45 g, 0.217 mmol), and DMAP solution (0.80 g, 0.215 mmol). The reaction mixture was stirred at room temperature for 12 h and added dropwise into 200 mL of dry Et_2O to form an orange precipitate. The complex was purified on an ion-exchange resin column of Sephadex-CM C-25 by eluting with an aqueous solution of 0.1 M NH_4Cl and phosphate buffer, pH 7.0. The product was collected on a fine glass frit as an orange precipitate after metathesis to the PF_6^- salt

(21) Dupray, L. M.; Meyer, T. J. *Inorg. Chem.* **1996**, *35*, 6299−6307.
(22) Kajita, T.; Friesen, D. A.; Danielson, E.; Meyer, T. J. *Inorg. Chem.* **1998**, *37*, 2756−2762.

Scheme 1

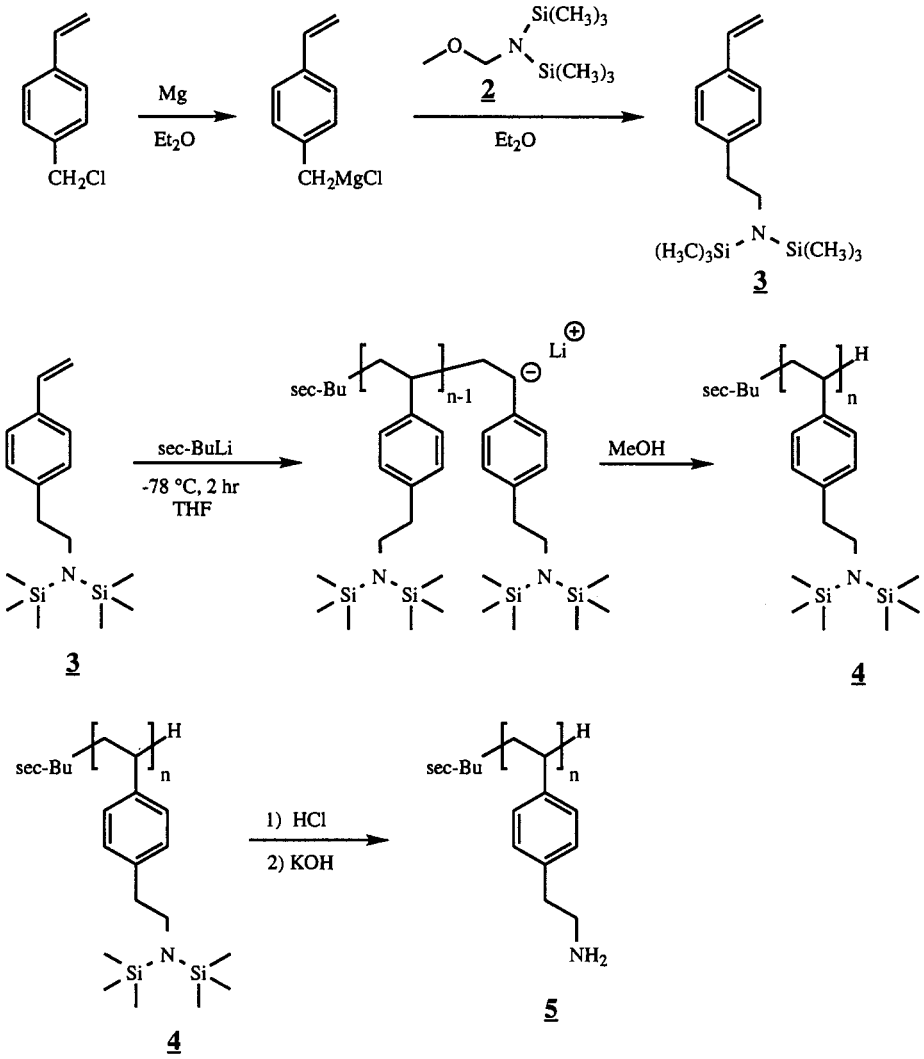

by treatment with aqueous ammonium hexafluorophosphate. The product was washed with several portions of cold distilled water and diethyl ether and dried in vacuo. ^{1}H NMR (δ (ppm), CD_3CN): 8.75 (s, 1H, bpy H6), 8.2−8.6 (m, 5H, bpy H6), 7.1−7.9 (m br, 17H, C_6H_5 and bpy H_3 H_5), 6.85 (dd overlapped, 2H, H_X), 6.32 (d, 2H, H_A), 6.72 (d, 2H, H_B), 3.66 (m br, 2H, $-NCH_2-$), 2.92 (m br, 2H, CH_2Ph), 2.2−2.5 (s overlapped, 9H, CH_3). FTIR (KBr): 3081, 3031, 2958, 2925, 2875, 2852, 1653, 1619, 1540, 1479, 1427, 842 cm^{-1}. UV−vis (CH_3CN): λ_{max} = 248, 296, 466 nm. Anal. Calcd for $C_{42}H_{37}F_{12}N_7OP_2Ru$: C, 50.2; H, 3.9; N, 8.9. Found: C, 49.6; H, 3.9; N, 8.5.

Results

Synthesis. The parent polymer, poly[4-(2-aminoethyl)-styrene] (**5**), used in the preparation of the macromolecular assemblies was synthesized by modification of a living anionic polymerization procedure reported by Nakahama and co-workers, Scheme 1.[20] The key to the polymerization is protection of the amine functional groups which would otherwise react with the living carbanion during polymerization. The trimethylsilyl group is suitable for protection of the amine, since the N−Si bond is stable to organolithium reagents used as initiators and can be easily cleaved under mild acidic conditions.[20]

The trimethylsilyl polymer (**4**) is atactic as shown by broad resonances in ^{13}C NMR spectra. The average number of repeat units was determined by gel permeation chromatography to be $n \approx 18$ with a molecular weight distribution of $\bar{M}_W/\bar{M}_n = 1.10$. The number of repeat units was assumed to be the same for the deprotected form of the polymer (**5**).

The polypyridyl complexes were added to **5** by amide coupling by using a controlled amount of complex and stoichiometric amounts of a mixture of peptide coupling reagents in dry DMF at room temperature.[23] Unreacted amines were converted into acetyl amide groups by reaction of the partially loaded polymers with acetic anhydride in acetonitrile. Fully loaded macromers were prepared by using an excess of **6**, Scheme 2.

The mixed polymer {p-PS-$CH_2CH_2NHCO[-bRu^{II}(bpy)_2]_{15.3}[-bRu^{II}(vbpy)_2]_{2.7}\}(PF_6)_{36}$ (**7**) was prepared by amide coupling first to 0.85 equiv of $[Ru^{II}(bpy)_2(4\text{-}CO_2H\text{-}4'\text{-}CH_3bpy)](PF_6)_2$. The degree of loading at this point can be determined experimentally by treating a small portion with acetic anhydride and comparing the ^{1}H NMR ethylene protons α to the amide nitrogen (~3.25 ppm) to ethylene protons (~3.50 ppm) on the branches containing the bound Ru^{II} complex. In the second amide coupling reaction, excess **6** was used to ensure complete loading of the remaining amine groups.

The monomeric analog of the macromer, $[Ru^{II}(vbpy)_2(4\text{-}CH_3\text{-}4'\text{-}(CONHCH_2CH_2Ph)bpy)](PF_6)_2$ (**8**), was prepared by using

(23) Jones, J. *Amino Acid and Peptide Synthesis*; Oxford University Press: Oxford, 1992.

Scheme 2

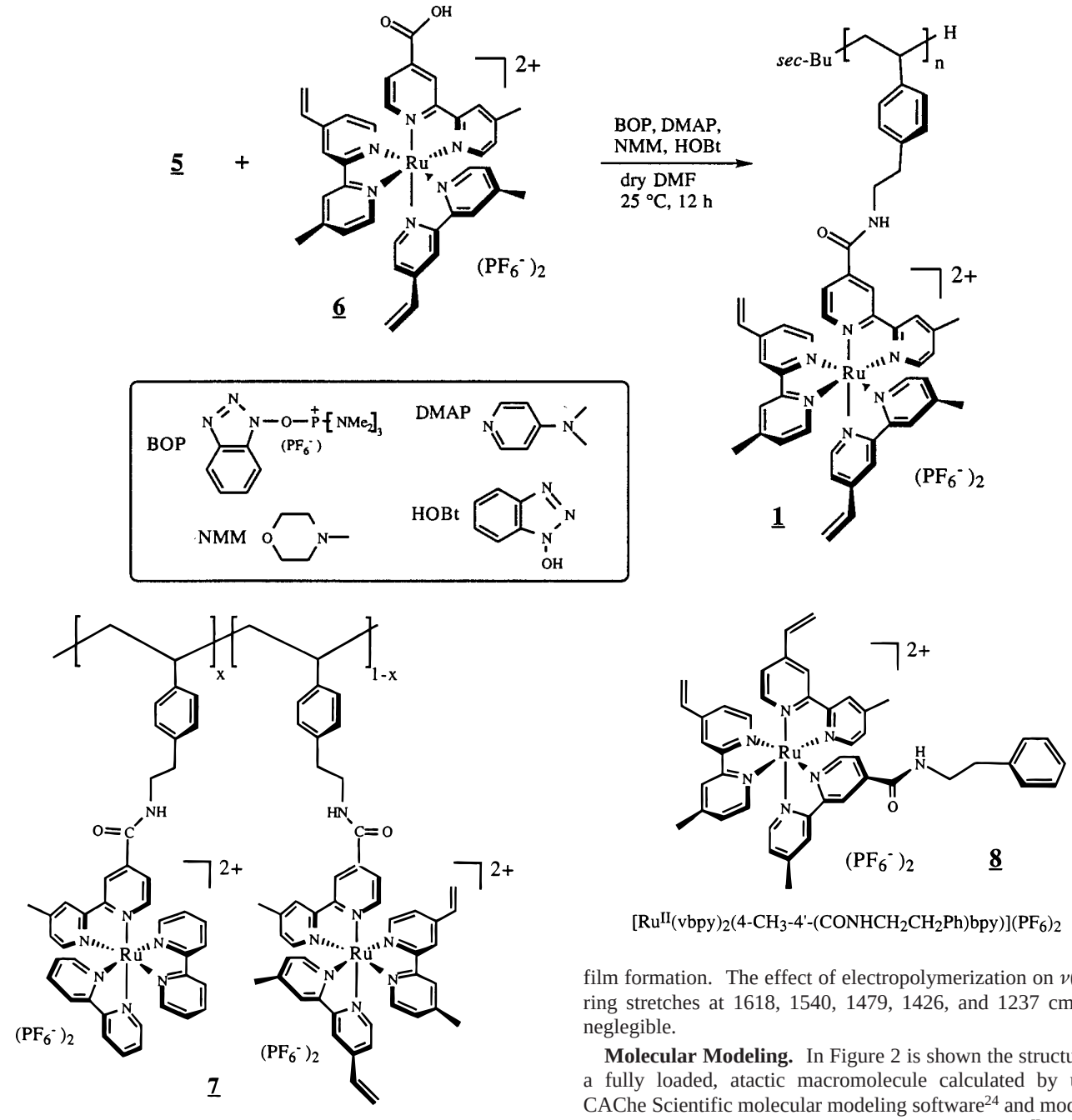

{p-PS-CH_2CH_2NHCO-[-$bRu^{II}(bpy)_2]_{15.3}$-[-$bRu^{II}(vbpy)_2]_{2.7}$}$(PF_6)_{36}$

the same reaction conditions as for the amide coupling but by substituting 2-phenylamine for poly[4-(2-aminoethyl)styrene].

FTIR Spectra. In Figure 1 are shown transmission FTIR spectra of (a) poly[4-(2-aminoethyl)-styrene], (b) [$Ru^{II}(vbpy)_2$(4-CO_2H-4′-CH_3bpy)]$(PF_6)_2$, and (c) {p-PS-CH_2CH_2NHCO[-$bRu^{II}(vbpy)_2]_{18}$}$(PF_6)_{36}$ (**1**) in KBr. Also shown is (d) the grazing angle FTIR spectrum of an electropolymerized film of **1** on a Au/Cr/SiO_2 electrode. Evidence of amide coupling is provided by the appearance of the ν(C=O) amide band at 1652 cm^{-1} in spectrum c and by the loss of bands due to amine (815 and 1596 cm^{-1}) and carboxylic acid groups (1718 cm^{-1}) which do appear in spectra a and b, respectively. The amide peak is retained after electropolymerization of the macromer, showing that the amide link is stable to reductive potential cycling during film formation. The effect of electropolymerization on ν(bpy) ring stretches at 1618, 1540, 1479, 1426, and 1237 cm^{-1} is neglegible.

Molecular Modeling. In Figure 2 is shown the structure of a fully loaded, atactic macromolecule calculated by using CAChe Scientific molecular modeling software[24] and modified MM2 parameters. In the calculation, each pendant Ru^{II} complex was treated as a sphere of diameter 14 Å and net 2+ charge. Because of the large molecular volumes of the complexes, large-amplitude displacements along the polymer backbone are restricted and the macromolecule is constrained to a nearly linear conformation. In the lowest energy structures, the center-to-center distance between nearest neighbors is ~18 ± 3 Å, with a close contact distance of ~4 Å between the peripheries of the complexes. Closer approaches, where electronic coupling would be enhanced, are accessible by local segmental motions. The distances are comparable to values found earlier for an ether-linked macromolecule, where the center-to-center distance was ~21 ± 2 Å.[25]

(24) *CAChe Scientific*, ver. 3.7; CAChe Scientific, Inc.: Beaverton, OR, 1992.

(25) Jones, W. E., Jr.; Baxter, S. M.; Strouse, G. F.; Meyer, T. J. *J. Am. Chem. Soc.* **1993**, *115*, 7363−7373.

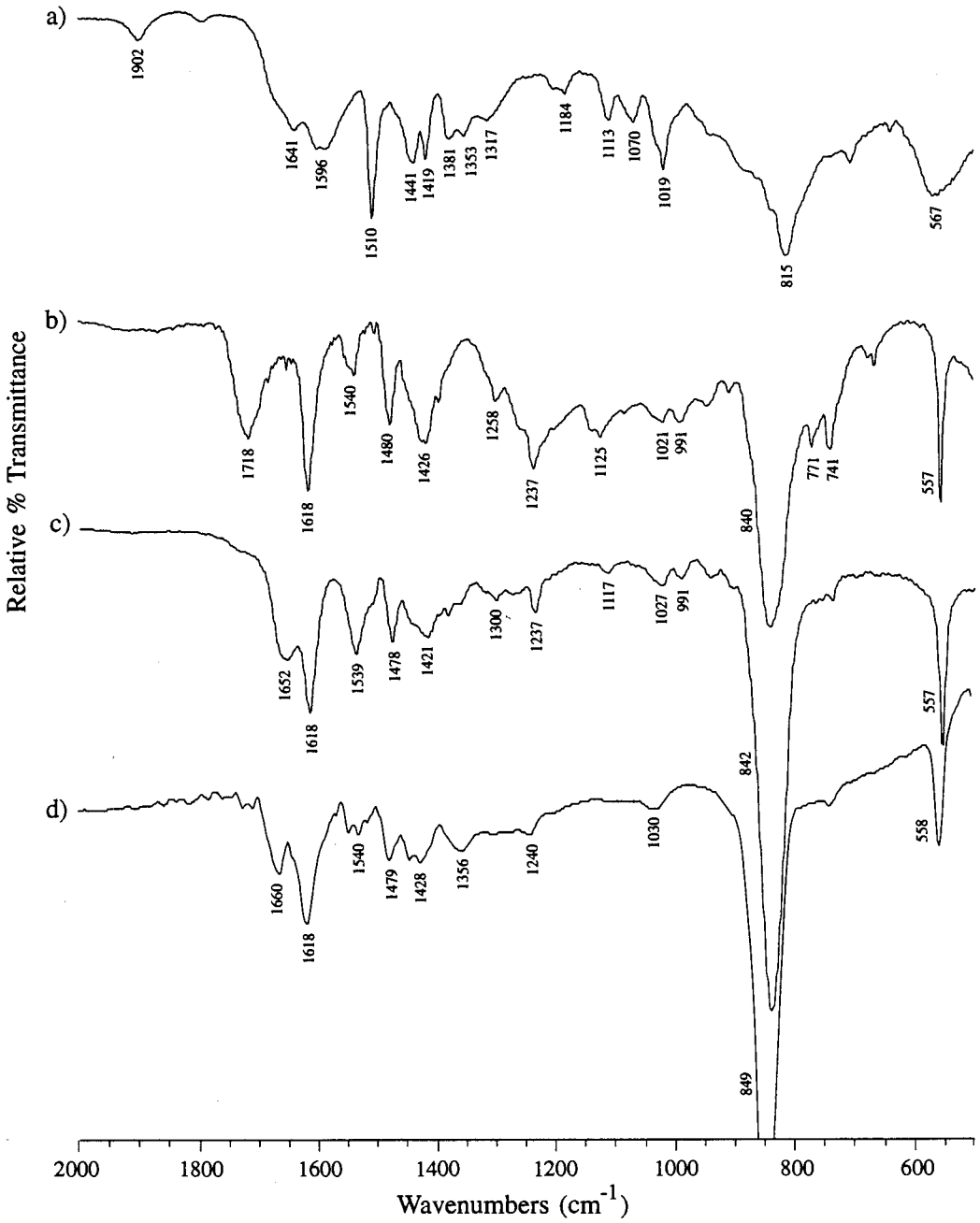

Figure 1. Transmission FTIR spectra of (a) poly[4-(2-aminoethyl)styrene], (b) $[Ru^{II}(vbpy)_2(4\text{-}CO_2H\text{-}4'\text{-}CH_3bpy)](PF_6)_2$ (**6**), and (c) $\{p\text{-}PS\text{-}CH_2CH_2NHCO[-bRu^{II}(vbpy)_2]_{18}\}(PF_6)_{36}$ (**1**) in KBr. (d) Spectral reflectance FTIR spectrum of an electropolymerized film of the macromer (poly-**1**) on a $Au/Cr/SiO_2$ electrode.

Electrochemistry. Formation of Thin Films. In Figure 3a is shown a cyclic voltammogram of **1** at a 0.12 cm^2 Pt disk in acetonitrile, 0.5 mM in Ru^{II} sites and 0.1 M in TBAH. A reversible wave for the $Ru^{III/II}$ couple occurs at 1.21 V vs SSCE, and three overlapping, one-electron, ligand-localized reductions between −1.3 and −1.8 V. A fourth wave at −1.90 V is presumably a second reduction at the amide-linked bipyridine.[26,27] $E_{1/2}$ values are listed in Table 1.

Thin polymeric films of the macromers and model complex were deposited on a variety of conducting substrates from acetonitrile solutions 0.25−1.0 mM in Ru^{II} sites and 0.1 M in TBAH. Polymerizations were carried out by repeatedly cycling the potential of the working electrode between −0.5 and −1.8 V (vs SSCE) through the ligand-based bipyridine reductions. In Figure 3b is shown a series of electropolymerization scans of **1** on a 0.12 cm^2 platinum disk. Peak currents increase with each scan as successive layers of polymer are formed. The vbpy reduction waves shift slightly to more negative potentials due to conversion of the vinyl substituents to more electron donating alkane cross-links.

Cyclic voltammograms of the resulting film in fresh electrolyte solution are shown in Figure 3c,d, and $E_{1/2}$ values are presented in Table 1. The typical oxidative and reductive prewaves are less prominent after the first scan cycle within each region. The prewaves arise from charge trapping of isolated redox sites or structural changes that accompany counterion flow.[2]

Surface coverages (Γ in mol/cm^2 of the Ru^{II} complex) were determined by integrating the charge, Q, under the cathodic

(26) Tokel-Takvoryan, N. E.; Hemingway, R. E.; Bard, A. J. *J. Am. Chem. Soc.* **1973**, *95*, 6582−6589.
(27) Wallace, W. L.; Bard, A. J. *J. Phys. Chem.* **1979**, *83*, 1350−1357.

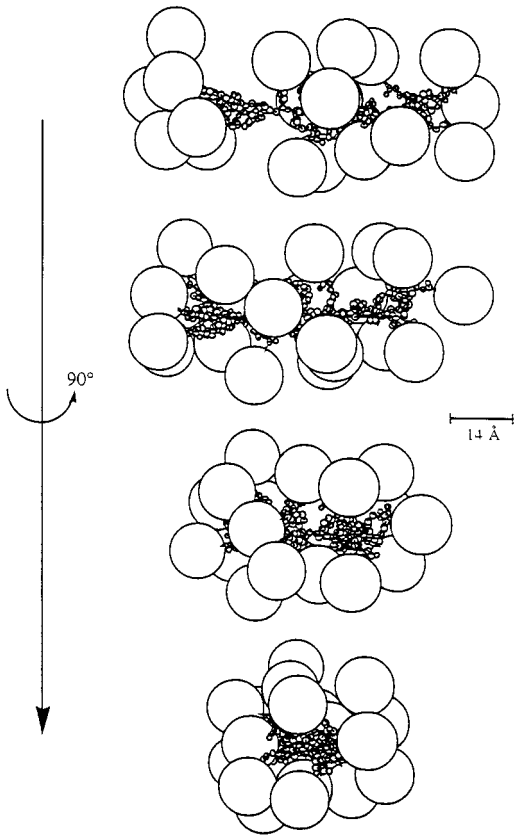

Figure 2. Molecular model of a fully loaded macromer, $n = 18$, calculated by using modified MM2 parameters. The complexes are shown as open spheres with carbon skeletons of the polymer backbone visible between them. The complexes were included in the calculation as spheres of diameter 14 Å and net 2+ charge. No attempt was made to include solvent or counterions. The various views are projections around an axis through the center at angles of 0°, 30°, 60°, and 90° with the last view looking down the polymer axis.

Table 1. $E_{1/2}$ Values vs SSCE in 0.1 M TBAH/CH_3CN at 25 °C in Solution (s) or Film (f)

	$E_{1/2}$ (V)				
complex, polymer, or film	$Ru^{III/II}$	red(1)	red(2)	red(3)	red(4)
macromer (**1**) (s)	1.21	−1.40	−1.50	−1.65	−1.90
poly-**1** (f)	1.23	−1.40	−1.53	−1.68	
model (**8**) (s)	1.22	−1.28	−1.48	−1.64	
poly-**8** (f)	1.24	− 1.28	− 1.50		
$[Ru^{II}(vbpy)_3](PF_6)_2$ (s)	1.13	− 1.37	− 1.52	− 1.74	
poly$[Ru^{II}(vbpy)_3](PF_6)_2$ (f)	1.18	−1.40	−1.57		
$[Ru^{II}(bpy)_3](PF_6)_2$ (s)	1.35	−1.33	−1.52	−1.76	−2.4

wave of the reversible $Ru^{III/II}$ couple by using eq 1 in which $n = 1$, F is Faraday's constant, and A is the measured geometric area of the electrode. Baseline corrections and determination

$$\Gamma = \frac{Q}{nFA} \tag{1}$$

of Q by numerical integration utilized a cubic-spline interpolation routine.[28,29] The amount of polymer deposited could be controlled by varying the concentration of the monomer in the solution used for electropolymerization, the reductive potential limits, the potential scan rate, and the number of polymerization cycles. Relative rates of electropolymerization under comparable conditions were $[Ru^{II}(vbpy)_3]^{2+}$ > [{p-PS-CH_2CH_2-NHCO[−b$Ru^{II}(vbpy)_2]_{18}$}]$^{36+}$ > $[Ru^{II}(vbpy)_2$(4-CH_3-4′-(CONH-CH_2CH_2Ph)bpy)]$^{2+}$. Electropolymerization of {p-PS-CH_2CH_2-NHCO[−b$Ru^{II}(bpy)_2]_{1.5.3}$[−b$Ru^{II}(vbpy)_2]_{2.7}$}$(PF_6)_{36}$ (**7**) was approximately 25× slower than for **1**. To achieve surface coverages of ca, $\times 10^{-9}$ mol/cm^2 required monomer solutions 1−2 mM in Ru^{II} sites and >40 reductive scans to −1.8 V.

The diffusion coefficient of **1** in acetonitrile, 0.1 M in TBAH, as measured by chronoamperometry,[30] was $D_s = 2.1 \times 10^{-5}$ cm^2/s. The measured value for $[Ru^{II}(bpy)_3](PF_6)_2$ is $D_s = 1.4 \times 10^{-6}$ cm^2/s under the same conditions.[31]

SEM and AFM Analyses of Film Morphology. In Figure 4 are shown scanning electron micrographs of electropolymerized films of the model complex **8** and the macromer **1** on SiO_2/Cr/Au electrodes, both $\Gamma \approx 5 \times 10^{-9}$ mol/cm^2. The film formed from **8** is essentially featureless, while the macromer film is rough, appearing to be composed of small spheres ∼0.5 μm in diameter.

Tapping mode atomic force microscopy (AFM) images of films on highly oriented pyrolytic graphite (HOPG) are shown in Figure 5. Contact mode AFM measurements in air proved inadequate for image acquisition due to film damage caused by the attractive forces between the tip and sample.[32,33] Root-mean-square (rms) surface roughnesses, R_q, were calculated from eq 2, in which z_i is the height of an individual point, $\bar{z}$ is the average height of all points in the image, and N is the total number of points in the image.[34] Values of R_q determined by

$$R_q = \sqrt{\frac{\sum (z_i - \bar{z})^2}{N}} \tag{2}$$

this method were 0.3 nm for bare HOPG, 15 nm for poly-$[Ru^{II}(vbpy)_2$(4-CH_3-bpy-$CONHCH_2CH_2Ph)]^{2+}$ ($\Gamma = 3.9 \times 10^{-9}$ mol/cm^2), and 200 nm for poly-**1** ($\Gamma = 5.2 \times 10^{-9}$ mol/cm^2).

Monolayer Adsorption of Macromers. The macromer of the non-vinyl-containing polymer, {p-PS-CH_2CH_2NHCO[−b$Ru^{II}(bpy)_2]_{18}$}$(PF_6)_{36}$, adsorbs on platinum by soaking the electrode in dilute acetonitrile solutions. There was no evidence of adsorption of $[Ru^{II}(vbpy)_3](PF_6)_2$ or $[Ru^{II}(vbpy)_2$(4-CH_3-4′-(CONHCH_2CH_2Ph)bpy)$](PF_6)_2$ under the same conditions.

An estimated monolayer coverage for 14 Å spheres is $\sim 1 \times 10^{-10}$ mol/cm^2.[35] From Figure 2, close packing of the macromer on the surface would result in the introduction of 2−3 redox sites per unit area, and the observed Γ of 1.4×10^{-10} mol/cm^2 is consistent with monolayer or submonolayer coverage. With **1** at 0.5 mM in Ru^{II} sites in the external solution, coverage was complete within 2 min. On a 0.02 cm^2 Pt disk in 0.1 M TBAH/CH_3CN, $E_{1/2}(Ru^{III/II}) = 1.31$ V vs SSCE with $\Delta E_{peak} \sim 0$ V, consistent with a surface-bound couple.[36] The monolayer was

(28) Chapra, S. C.; Canale, R. P. *Numerical Methods for Engineers*; McGraw-Hill: New York, 1985.
(29) Coia, G. M. Ph.D. Dissertation, University of North Carolina at Chapel Hill, 1996.
(30) Bard, A. J.; Faulkner, L. R. *Electrochemical Methods*; John Wiley & Sons: New York, 1980.
(31) Diffusion coefficients were calculated by using the Cottrell equation and slopes of j vs $t^{-1/2}$ plots from chronoamperometric data. Because n and C_S are to the first power in the Cottrell equation, and given the well defined structure of the fully loaded, parent polymer, it is valid to assume $n = 1$, provided that C_S is taken to be the formula weight of one repeat unit.
(32) Grigg, D. A.; Russel, P. E.; Griffith, J. E. *J. Vac. Sci. Technol. A* **1992**, *10* (4), 680−683.
(33) Thundat, T. *Surf Sci* **1993**, *294*, L939−L943.
(34) Musselman, I. H.; Gray, K. H.; Leasure, R. M.; Meyer, T. J.; Linton, R. W. *Microbeam Anal.* **1993**, *2*, 297−310.
(35) Meyer, G. J.; Pfenning, B. W.; Schoonover, J. R.; Timpson, C. J.; Wall, J. F.; Wall, C. G.; Ou, W.; Erickson, B. W.; Bignozzi, C. A.; Meyer, T. J. *Inorg. Chem.* **1994**, *33*, 3952.
(36) Murray, R. W. In *Electroanalytical Chemistry*; A. J. Bard, Ed.; Marcel Dekker: New York, 1984; Vol. 13; pp 191−368.

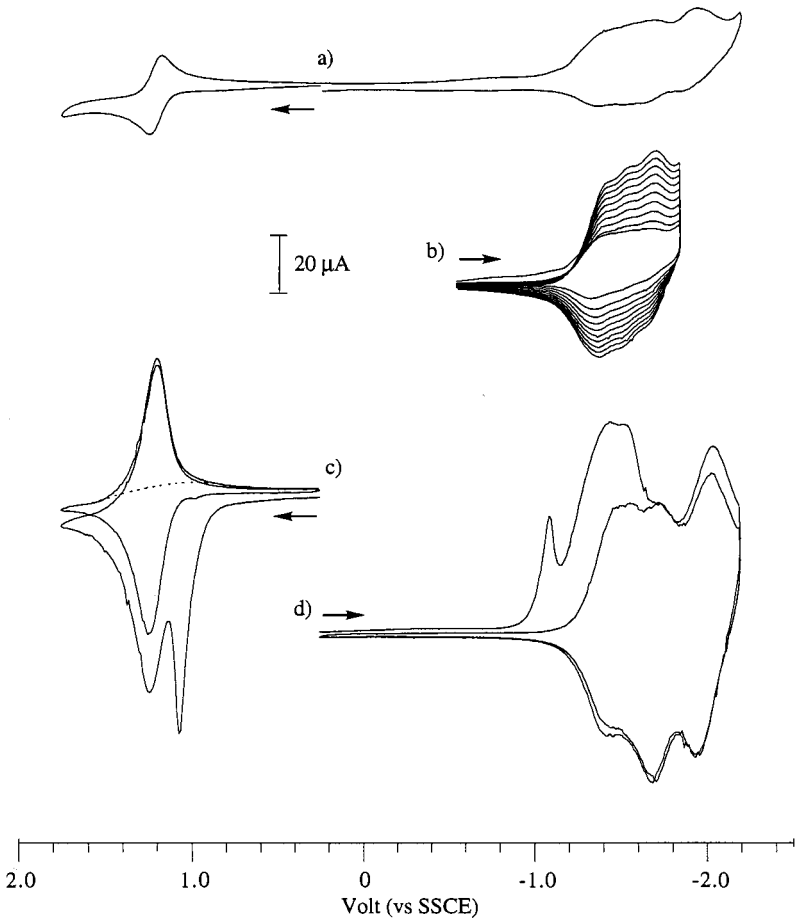

Figure 3. (a) Cyclic voltammogram of **1** at a 0.12 cm^2 Pt disk in 0.1 M TBAH/CH_3CN, 0.5 mM in Ru^{II} sites, vs SSCE. (b) Reductive electropolymerization of the macromer by repeated potential scans between −0.5 and −1.8 V. (c) Anodic and (d) cathodic cyclic voltammograms of the resulting film ($\Gamma = 8.2 \times 10^{-9}$ mol/cm^2) in fresh electrolyte solution not containing the macromer. In all cases, the scan rate was 100 mV/s.

stable to repeated anodic cycling, but over 50% of the current for the $Ru^{III/II}$ couple was lost after three reductive cycles to −1.8 V.

Charge Transport within the Films. Charge transfer diffusion coefficients, D_{app}, were measured for poly-**1** and poly-$[Ru^{II}(vbpy)_3](PF_6)_2$ by potential step chronoamperometry on films from $\Gamma = (0.7-1.8) \times 10^{-9}$ mol/cm^2 on 0.12 cm^2 platinum disks in 1.0 M $LiClO_4/CH_3CN$.[2,37,38] The potential was stepped 100 mV to either side of the $Ru^{III/II}$ couple. Current−time transients were analyzed by using the Cottrell equation, eq 3,[30] with D_{app} the diffusion coefficient in cm^2 s^{-1}, j the current density in A/cm^2, t the time in s, and C_f the molar concentration of redox sites in the films. Plots of j vs $1/t^{1/2}$ were linear from

$$j = \frac{nFD_{app}{}^{1/2}C_f}{\pi^{1/2}t^{1/2}}$$

4 to 10 ms, over which 60% of the total charge was passed. Values for $D_{app}{}^{1/2}C_f$ and D_{app}, estimated by assuming $C_f = 1.3$ M, are reported in Table 2.[2,39,40]

The extent of film electroactivity was investigated by using spectroelectrochemical measurements of poly-**1**, $\Gamma = 2.0 \times 10^{-8}$ mol/cm^2, on an optically transparent ITO electrode immersed in 0.1 M TBAH/CH_3CN. The potential of the electrode was initially held at 0.8 V and then stepped to 1.8 V, where it was held for 5 min. From the decrease in absorbance at $\lambda_{max} =$ 468 nm, the extent of Ru^{II} oxidation to Ru^{III} was ∼87%.[41]

Rotating Disk Voltammetry. Diffusion of $[Os^{II}(dmb)_3]^{2+}$ (dmb is 4,4′-dimethyl-2,2′-bipyridine) through the films was measured by rotating-disk voltammetry. Current−potential waveforms were acquired as a function of rotation rate (95−513 rad/s) in CH_3CN 1.0 mM in Os^{II} and 0.1 M in TBAH at a bare Pt disk and a disk coated with poly-**1**, $\Gamma = 4.3 \times 10^{-9}$ mol/cm^2.

At the bare Pt disk, $E_{1/2} = 0.63$ V vs SSCE for the $Os^{III/II}$ couple with $D_s = 8.1 \times 10^{-6}$ cm^2/s determined from the Levich equation, eq 4,[30] and the slope of a plot of j_{lim} vs $\omega^{1/2}$. In eq 4, $n = 1$, A is the geometric area of the electrode, ν is the kinematic viscosity (4.39×10^{-3} cm^2/s at 25 °C),[42] ω is the rotation rate, and C_s is the concentration of electroactive species S in the external solution.

$$j_{lim} = 0.62nFD_s{}^{2/3}\nu^{-1/6}\omega^{1/2}C_s \qquad (4)$$

At the film-coated electrode, the potential for the $Os^{III/II}$ couple is shifted near the onset for the $Ru^{III/II}$ surface wave at $E_{1/2} =$

(37) Daum, P.; Lenhard, J. R.; Rolison, D.; Murray, R. W. *J. Am. Chem. Soc.* **1980**, *102*, 4649−4653.
(38) Daum, P.; Murray, R. W. *J. Phys. Chem.* **1981**, *85*, 389−396.
(39) Leidner, C. R.; Murray, R. W. *J. Am. Chem. Soc.* **1984**, *106*, 1606−1614.
(40) McCarley, R. L.; Thomas, R. E.; Irene, E. A.; Murray, R. W. *J. Electrochem. Soc.* **1990**, *137*, 1485−1490.
(41) Buttry, D. A.; Anson, F. C. *J. Am. Chem. Soc.* **1982**, *104*, 4824−4829.
(42) *CRC Handbook of Chemistry and Physics*, 67th ed.; Weast, R. C., Ed.; CRC Press: West Palm Beach, 1986, pp F36−F38.

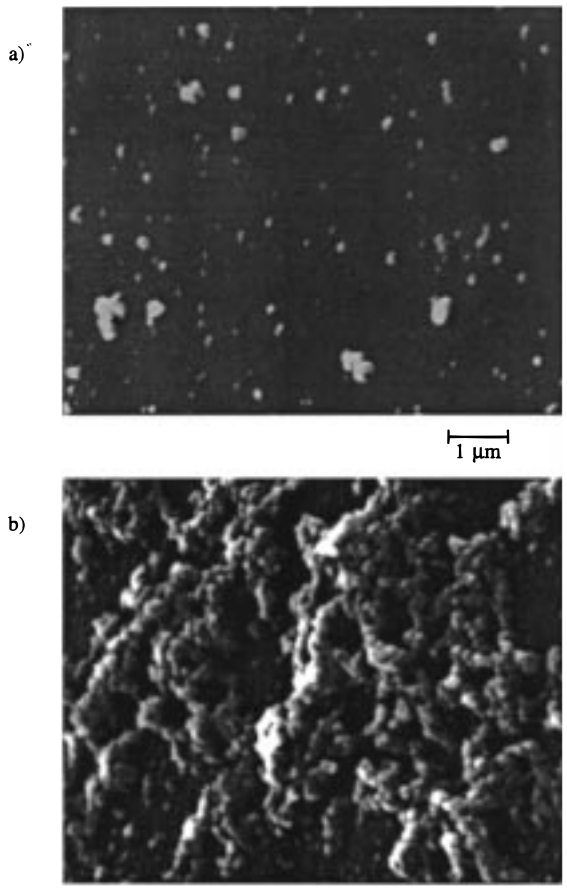

Figure 4. High-resolution SEM images of electropolymerized films from (a) **8** to give poly[Ru^{II}(vbpy)$_2$(4-CH_3-4′-($CONHCH_2CH_2Ph$)bpy)]-(PF_6)$_2$ and from (b) **1** to give poly{p-ps-CH_2CH_2NHCO[−bRu^{II}-(vbpy)$_2$]$_{18}$}(PF_6)$_{36}$, both on Au/Cr/SiO_2 with $\Gamma \approx 5 \times 10^{-9}$ mol/cm^2.

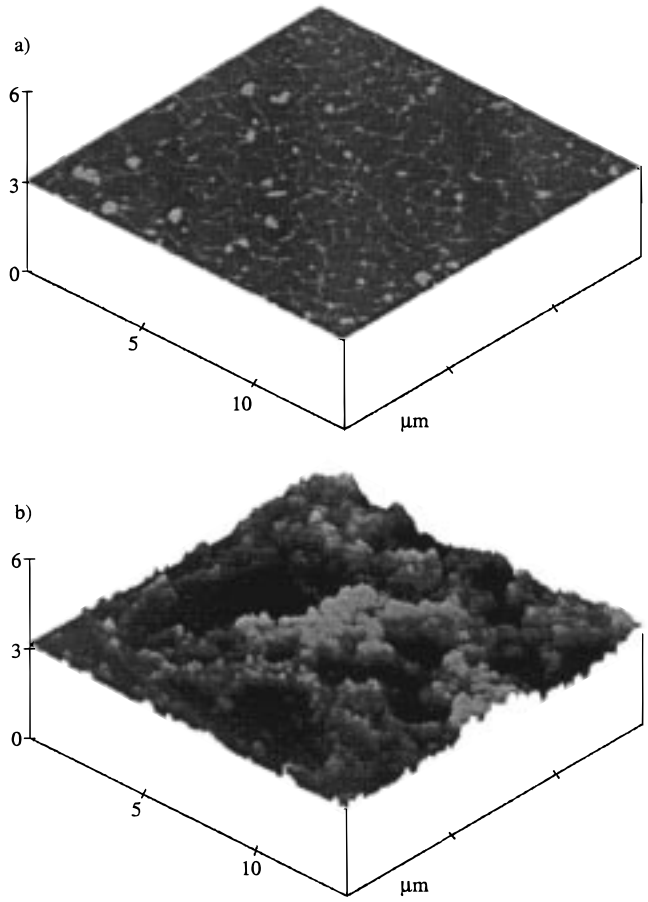

Figure 5. Three-dimensional tapping mode AFM images (12.5 × 12.5 μm) of electropolymerized films of (a) the model, poly[Ru^{II}(vbpy)$_2$(4-CH_3-4′-($CONHCH_2CH_2Ph$)bpy)](PF_6)$_2$, R_q = 20 nm; and (b) the macromer, poly{p-PS-CH_2CH_2NHCO[−bRu^{II}(vbPy)$_2$]$_{18}$}(PF_6)$_{36}$, R_q = 0 02 μm. Both films were grown on freshly cleaved HOPG under conditions that gave equivalent surface coverages of $\Gamma \approx 5 \times 10^{-9}$ mol/cm^2.

1.23 V. This is consistent with mediated oxidation by the $Ru^{III/II}$ couple in the film due to slow diffusion of $[Os(dmb)_3]^{2+}$ through the film.

Photophysical Measurements. In Figure 6 are shown room temperature absorption, emission, and excitation spectra of (a) macromer **1** in CH_3CN and (b) an electropolymerized film of poly-**1** ($\Gamma = 1.5 \times 10^{-8}$ mol/cm^2) on an optically transparent ITO electrode immersed in deaerated CH_3CN. In the UV (<350 nm), the absorption spectrum of the macromer in solution is dominated by $\pi \rightarrow \pi^*$ bipyridine and polystyrene bands. These are not observed on ITO because of its high-energy cutoff at 350 nm. In the visible, dπ(Ru^{II}) → π^*(bpy) metal-to-ligand (MLCT) bands appear with maxima at 468 nm and shoulders at ~440 nm. Spectral data are summarized in Table 3.

Transient emission measurements were conducted with 457 nm excitation (~90 μJ/cm^2 per pulse) and monitoring at 680 nm. Solution samples were optically dilute (ca. 10 μM) and bubble deoxygenated with Ar for a minimum of 15 min. Emission from film samples on ITO immersed in CH_3CN were also measured with 457 nm excitation (5−25 μJ/mm^2 per pulse). The same results were obtained whether or not the external solution had been deaerated.

Emission decays were fitted by a modified Levenberg−Marquardt nonlinear least-squares routine[43−45] to the single exponential expression in eq 5, or to the sum of two weighted exponentials in eq 6.[46] $I(t)$ is the emission intensity at time t,

$$I(t) = A \exp[-(t/\tau_1)] \quad (5)$$

$$I(t) = A \exp[-(t/\tau_1)] + (1 - \text{Å}) \exp[-(t/\tau_2)] \quad (6)$$

A is the fraction of emission by the first component, and τ_1 and τ_2 are the lifetimes of the components. For consistency, each data set was fitted over the same temporal range (10−350 ns) after the transient maximum was reset to 0 ns. The biexponential fits provided satisfactory mathematical representations of the emission decay data, but do *not* imply that there are two discrete, emitting Ru^{II}* sites. More likely there is a distribution of lifetimes with the long and short components providing reasonable estimates of the distribution extremes and their relative contributions. Mean lifetimes were calculated by using eq 7 and are reported in Table 3.

$$\bar{\tau} = \sum_{i=1}^{2} A_i \tau_i \quad (7)$$

In Figure 7 is shown a typical luminescent decay trace from poly-**1** on an ITO electrode, along with the biexponential fit and residuals. Lifetime data are summarized in Table 3.

(43) Levenberg, K. *Q. Q. Appl. Math.* **1944**, *2*, 164−168.
(44) Marquardt, D. W. *Appl. Math.* **1963**, *11*, 431.
(45) Seber, G. A.; Wild, C. *J. Non-Linear Regression*; Wiley: New York, 1987.
(46) Demas, J. N. *Excited State Lifetime Measurements*; Academic: New York, 1983.

Table 2. D_{app} in Polymeric Films from Chronoamperometry in 1.0 M $LiClO_4/CH_3CN$ at 25 °C

film	Γ ($\times 10^{-8}$ mol/cm^2)	$D_{app}^{1/2}C_f$ ($\times 10^{-8}$ mol/cm^2 s$^{1/2}$)	D_{app}[a] ($\times 10^{-8}$ cm^2/s)
poly{p-PS-CH_2CH_2NHCO[+bRu^{II}(vbpy)$_2$]$_{18}$}$(PF_6)_{36}$	1.74	3.37	6.72
	1.54	3.32	6.52
	1.17	2.95	5.04
	0.76	1.98	2.31
	0.72	1.75	1.81
		av: 2.67 ± 0.76	4.6 + 2.3
poly[Ru^{II}(vbpy)$_3$]$(PF_6)_2$	1.69	1.48	1.29
	1.49	2.26	3.02
	1.19	1.11	0.72
	0.78	1.14	0.76
		av: 1.49 ± 0.54	1.4 ± 1.1

[a] Calculated assuming a redox-site concentration of $C_f = 1.3$ M.

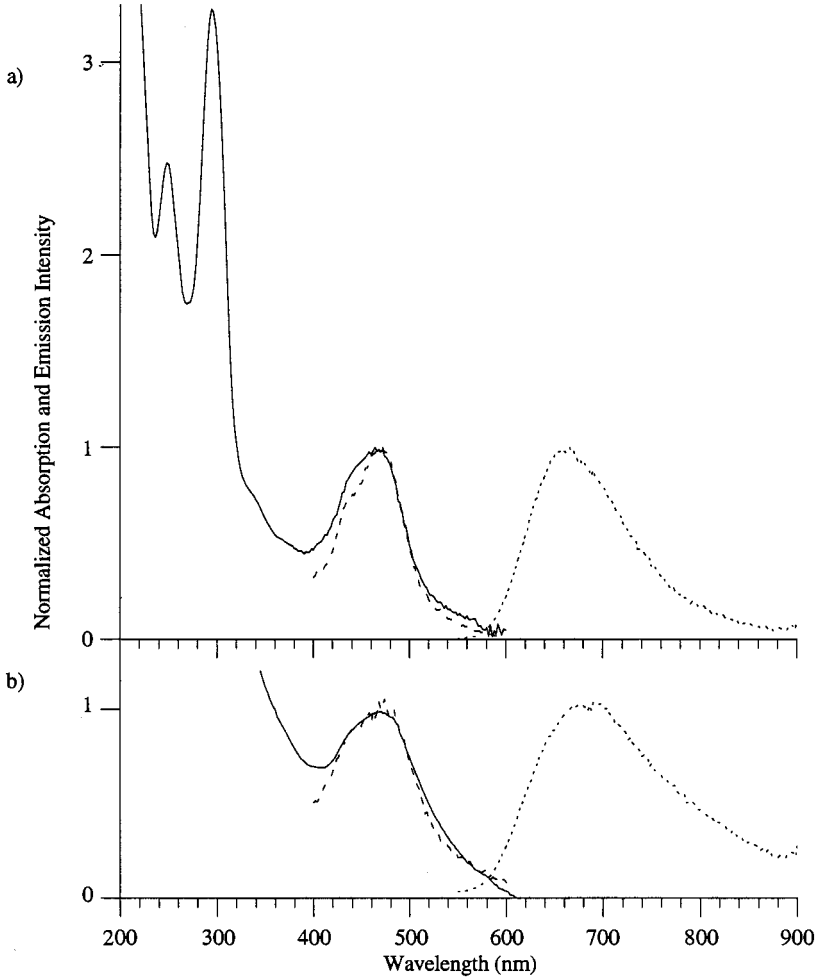

Figure 6. Room temperature absorption (—), excitation (– – –), and emission (---) spectra for (a) macromer (**1**) in acetonitrile and (b) an electropolymerized film of the macromer (poly-**1**, $\Gamma = 1.5 \times 10^{-8}$ mol/cm^2) on an optically transparent ITO electrode immersed in acetonitrile.

Surface coverages of the films ranged from 1×10^{-9} to 5×10^{-9} mol/cm^2. Over this range, lifetimes appeared independent of film thickness. Consistent lifetime values for the same films were obtained over a period of several months, indicating that the films were stable to long-term storage.

Discussion

As noted in the Introduction, there is by now an extensive literature on the electropolymerization of vinyl- and pyrrole-containing metal complexes. This chemistry has led to the preparation of a variety of novel film-based structures. This includes heterogeneous, multilayered structures containing spatially discrete, redox-active regions, and molecular composites with different molecules in the same region. Procedures have been described for imaging and the creation of vertical columnar structures and active microstructures for catalysis, electrochromism, and "molecular filtering".[16,47−49]

Electropolymerization of molecular assemblies opens a new dimension in this chemistry. In preformed assemblies, it is

(47) Gould, S.; O'Toole, T. R.; Meyer, T. J. *J. Am. Chem. Soc.* **1990**, *112*, 9490−9496.
(48) Leasure, R. M.; Moss, J. A.; Meyer, T. *J. Inorg. Chem.* **1994**, *33*, 1247−1248.
(49) Gould, S.; Gray, K. H.; Linton, R. W.; Meyer, T. J. *J. Phys. Chem.* **1995**, *99*, 16052−18058.

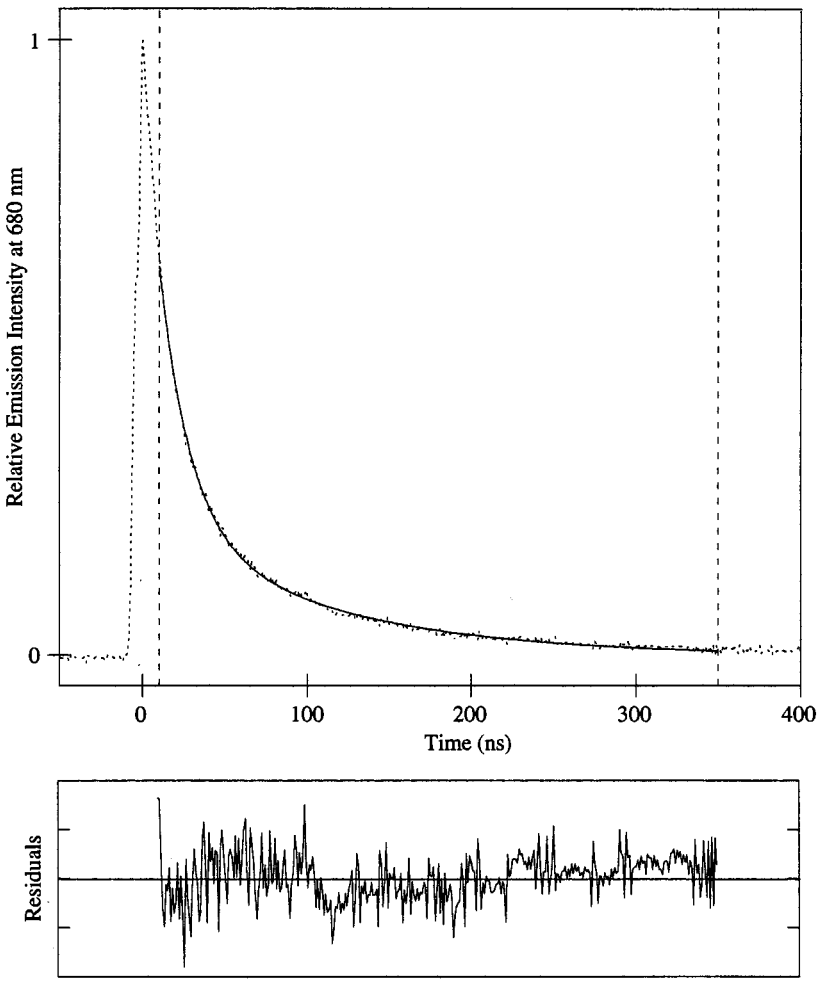

Figure 7. Emission decay trace for an electropolymerized film of poly-**1** ($\Gamma = 1.5 \times 10^{-8}$ mol/cm^2) on an ITO electrode immersed in CH_3CN monitored at 680 nm following 457 nm excitation ($\sim$10 νJ/mm^2 per pulse). The overlay is the fit to the decay between 10 and 350 ns (indicated by the vertical dashed lines) calculated by using eq 7 and the parameters in Table 3. The residuals to the fit are shown in the lower box.

Table 3. Photophysical Properties in CH_3CN at 25 °C

	λ_{abs}^{MLCT} (nm)	λ_{em} (nm)	τ_1 (A)	τ_2	$\bar{\tau}$
	Solution				
$[Ru^{II}(bpy)_3](PF_6)_2$	451	620	855		
$[Ru^{II}(vbpy)_3](PF_6)_2$	466	661	1620		
model (**8**)	470	662	1153		
macromer (**1**)	468	662	1144 (0.65)	267	837
mixed macromer (**7**)	466	645	1250 (0.57)	320	850
	Film				
poly$[Ru^{II}(vbpy)_3](PF_6)_2$	460	690	110 (0.15)	20	34
model (poly-**8**)	470	700	106 (0.17)	18	33
macromer (poly-**1**)	468	678	124 (0.19)	19	39
mixed macromer (poly-**7**)	466	662	131 (0.36)	23	62
poly-**1** (removed from electrode in a SiO_2 sol−gel)			137 (0.26)	22	52

possible to introduce multiple functions in spatially controlled positions in the molecular array. By controlling the site or sites containing polymerizable groups, it may be possible to control internal microstructure and micromorphology within the films.

In this paper we describe the preparation and properties of polymeric films based on reductive electropolymerization of vinyl-containing "macromers". The polymeric backbone was prepared by anionic polymerization, offering the advantage of low polydispersity and a relatively narrow distribution of molecular weights. The existence of the amino groups provides a general approach to derivatization based on standard amide coupling to acid-derivatized, redox-active, or photochemically active molecular modules. In this case, introduction of 4-methyl-4′-vinyl-2,2′-bipyridine (vbpy) ligands bound to Ru^{II} creates macromers and the ability to undergo electropolymerization. It is notable that electropolymerization and film formation also occur for $\{p\text{-PS-}CH_2CH_2NHCO[-bRu^{II}(bpy)_2]_{15.3}[-bRu^{II}(vbpy)_2]_{2.7}\}(PF_6)_{36}$ (**7**), in which only 15% of the attached complexes contain vinyl groups. This shows that it is possible to use a limited number of vinyl-containing units as structural elements for film formation.

Reductive electropolymerization of vinyl-containing metal complexes occurs by a radical-anion, chain-propagating mechanism as electrons are added to the π^* orbitals of the vbpy ligands.[3,50,51] Films form at the electrode/solution interface as the extent of oligomerization and cross-linking increase, de-

creasing the solubility of the growing network. The amount of unreacted vinyl substituent within the macromeric films and the extent of intramolecular cross-linking, i.e., between adjacent Ru^{II} sites on the same polystyrene backbone, are not known.

Film Morphology. On the basis of the AFM measurements, the rms surface roughness of the macromeric films is approximately 10× greater than that of films of similar coverages ($\Gamma \approx 5 \times 10^{-9}$ mol/cm^2) prepared from $[Ru^{II}(vbpy)_2(4\text{-}CH_3\text{-}4'\text{-}(CONHCH_2CH_2Ph)bpy)](PF_6)_2$ (**8**). SEM images reveal that the macromeric films are composed of aggregates of spheres with diameters of ca. 0.5 μm. The evidence for nodular growth is consistent with rapid cross-linking of the macromers and formation of insoluble clusters of the polymer. Similar observations have been reported by Murray and co-workers on *thick* films ($\Gamma > 1 \times 10^{-8}$ mol/cm^2) of poly$[Os^{II}(bpy)_2(vpy)_2]^{2+}$ (bpy is 2,2′-bipyridine, vpy is 4-vinylpyridine) and attributed to precipitation of sparingly soluble oligomers that form in solution away from the electrode surface.[40] For the macromers, dendritic film growth is accelerated due to the large number of polymerizable sites ($2n = 36$ sites) and the fact that the macromers are themselves "oligomers".

Intrafilm Electron Transfer. Charge transport within poly-**1**, measured by chronoamperometry, gave an average diffusion coefficent of $D_{app} = 4.6 \times 10^{-10}$ cm^2 s^{-1}. This shows that intrafilm electron transfer in the porous polymacromeric films is slightly enhanced compared to that in poly$[Ru^{II}(vbpy)_3]^{2+}$, where $D_{app} = 1.4 \times 10^{-10}$ cm^2 s^{-1}. This result, as well as the fact that >85% oxidation to Ru^{III} occurs at 1.8 V, demonstrates that $Ru^{II} \rightarrow Ru^{III}$ oxidation is a well-defined process in the films. Counterion transport necessarily accompanies electron transfer, and either, or a combination of the two, can be rate determining. Detailed comparisons between the two types of films are difficult to make. One reason is the uncertainty associated with estimates of the film density. It is possible that the greater D_{app} for the electropolymerized, macromeric film may be due to enhanced counterion transport because of a more open local microstructure.

Film-Mediated Electron Transfer. On the basis of the rotating disk voltammetric results, direct oxidation of $[Os^{II}(dmb)_3]^{2+}$ by diffusion to electrodes coated with poly-**1** does not occur. The films effectively act as impermeable membranes to the large (~14 Å diameter) dications on the time scale of the experiment. Similar observations have been made for smooth electropolymerized films of poly$[Os^{II}(bpy)_2(vpy)_2](PF_6)_2$, where the permeabilities of bulky, dicationic complexes were found to be extemely low.[39] Given the open, dendritic growth revealed in the SEM and AFM images for poly-**1**, there must be an underlying, dense, homogeneous layer of polymer which blocks diffusion. It is plausible that the adsorbed monolayer or submonolayer of macromers on the electrode surface described in the Results provides a template for smooth film growth during deposition of the first few layers by reductive cycling.

The slopes of Levich plots for bare Pt and polymer-coated electrodes in the rotating-disk experiments were nearly identical, with zero intercepts in both cases. The enhanced microscopic roughness for poly-**1** has no effect on the observed current density, since the surface features (ca. 0.5 μm in diameter) are considerably smaller than the diffusion layer thickness, δ, which for rotating-disk voltammetry is given by eq 8.[36] From this equation, even at the fastest rotation rate, $\omega = 513$ rad/s, the

$$\delta = 1.61 D_S^{1/3} \nu^{1/6} \omega^{-1/2} \quad (8)$$

diffusion layer is 5.8 μm, larger than the surface features of the film by 10×.

Photophysics. Typical metal-to-ligand charge transfer (MLCT) emission is observed from the model complex and the Ru^{II} sites in the polymers. The emission energy for $[Ru^{II}(vbpy)_2(4\text{-}CH_3\text{-}4'\text{-}(CONHCH_2CH_2Ph)bpy)](PF_6)_2$ (**8**) in acetonitrile (662 nm) is lower than for $[Ru^{II}(bpy)_3]^{2+}$ (620 nm). Time-resolved resonance Raman measurements on related complexes show that the excited electron is on the amide-derivatized bipyridine.[11] The shift to lower energy for emission is caused by the lower π^* level in the amide-derivatized acceptor ligand and the substituent effects of the vinyl and methyl groups on the vbpy "spectator" ligands. They stabilize the excited state by electron donation.

Emission from **1** in acetonitrile also occurs at 662 nm. In the mixed macromer (**7**), emission is dominated by the $[-bRu^{II}(bpy)_2]^{2+}$ sites and occurs at 645 nm. Emission decays are nonexponential as found for other polystyrene-derivatized Ru^{II} polymers. The possible origins of the nonexponentiality have been discussed elsewhere.[21,22,25,52−55]

MLCT absorption bandshapes and maxima in electropolymerized films of the macromers on ITO are similar to those of the model complex and the polymers in solution. The absorption bands in the visible arise from overlapping $Ru^{II} \rightarrow$ (polyvbpy), $Ru^{II} \rightarrow$ (bpyCONH−) transitions. MLCT band energies are known to be medium dependent,[56] and the similarity in energies points to an instantaneous microenvironment in the films similar to CH_3CN as solvent.

By contrast, lifetimes and emission energies are considerably altered in the films. Emission bands are broader and shifted to lower energy. Emission decays are nonexponential and could be fitted to the biexponential function in eq 7. Average excited state decay times are decreased by more than 20-fold. Similar observations have been made in films of poly$[Ru(vbpy)_3]^{2+}$ compared to $[Ru(vbpy)_3]^{2+}$ in solution.[57] In those films, it was concluded that the photophysical properties can be explained by invoking dynamical energy transfer to low-energy trap sites which dominate emission at long times. The trap sites may originate from sites in the films where there is a structural basis for excited state−ground state interactions which decrease the excited state energy and the nonradiative lifetime.

Average lifetimes for poly-**1** were independent of incident light intensity from 5 to 25 μJ/mm^2 per pulse. Electrode quenching did not contribute significantly to excited state decay. This was shown by the similarity in lifetimes in electropolymerized films on ITO and with films physically removed from the electrode by attachment to a sol−gel matrix.[18] This was also shown to be the case in a previous study involving bilayer film structures of ITO/poly$[Zn^{II}(vbpy)_3]^{2+}$/poly$[Ru^{II}(vbpy)_3]^{2+}$,[57] in which the inner layer of poly$[Zn^{II}(vbpy)_3]^{2+}$ acts as an insulator between the electrode and the outer polymeric layer containing Ru^{II}.

(50) Elliott, C. M.; Baldy, C. J.; Nuwaysir, L. M.; Wilkins, C. L. *Inorg. Chem.* **1990**, *29*, 389−392.
(51) Guarr, T. F.; Anson, F. C. *J. Phys. Chem.* **1987**, *91*, 4037−4043.
(52) Strouse, G. F.; Worl, L. A.; Younathan, J. N.; Meyer, T. J. *J. Am. Chem. Soc.* **1989**, *111*, 9101−9102.
(53) Worl, L. A.; Strouse, G. F.; Younathan, J. N.; Baxter, S. M.; Meyer, T. J. *J. Am. Chem. Soc.* **1990**, *112*, 7571−7578.
(54) Younathan, J. N.; Jones, W. E., Jr.; Meyer, T. J. *J. Phys. Chem.* **1991**, *95*, 488−492.
(55) Baxter, S. M.; Jones, W. E., Jr.; Danielson, E.; Worl, L.; Strouse, G.; Younathan, J.; Meyer, T. J. *Coord. Chem. Rev.* **1991**, *111*, 47−71.
(56) Chen, P.; Meyer, T. J. *Chem. Rev.* **1998**, *98*, 1439−1477.
(57) Devenney, M.; Worl, L. A.; Gould, S.; Guadalope, A.; Sullivan, B. P.; Caspar, J. V.; Leasure, R. M.; Gardner, J. R.; Meyer, T. J. *J. Phys. Chem.* **1997**, *101*, 4535−4540.

The degree of cross-linking does have an effect on excited state decay, but it is slight. In the heavily cross-linked polymers, poly[$Ru^{II}(vbpy)_3$]$(PF_6)_2$, poly-**8**, and poly-**1**, there is relatively little difference between the short and long components to the measured lifetimes, Table 3. Average lifetimes in these films are on the order of 30-40 ns. In films of the mixed-complex macromer (poly-**7**) there are, on average, only 5.4 cross-link sites compared to 36 for the pure vinyl containing macromer. In this film, the CW emission energy decreases to 662 nm (15 100 cm^{-1}) compared to 645 nm (15 500 cm^{-1}) in solution, and the average lifetime increases 2-fold. Although this is not a dramatic increase, it demonstrates the importance of either composition and/or microenvironment on excited state decay. The effects on excited state lifetimes of compositional variations are currently under investigation. It is not yet clear if emission is dominated by the majority Ru-bpy sites or by the linked Ru-poly(vbpy) sites, and what role, if any, is played by intrastrand energy transfer and quenching by trap sites.

Acknowledgment. The authors gratefully acknowledge the Japan Synthetic Rubber Co., Ltd., and the U.S. Army Research Office under Grants No. DAAL03-90-G-0062 and DAAL03-92-G-D166 for financial support of this work. The authors also thank Dr. Michael O. Hunt for GPC measurements, Wallace A. Ambrose for SEM measurements, Dr. Wei Ou for AFM measurements, and Prof. Joseph M. DeSimone for insightful discussions about the polymer synthesis.

IC971279W